

# Floating probe for electron temperature and ion density measurement applicable to processing plasmas

Min-Hyong Lee, Sung-Ho Jang, and Chin-Wook Chung<sup>a)</sup>

*Department of Electrical and Computer Engineering, Hanyang University, 17 Haengdang-dong, Seongdong-gu, Seoul 133-791, Republic of Korea*

(Received 3 November 2005; accepted 13 April 2006; published online 13 February 2007)

A floating-type probe and its driving circuit using the nonlinear characteristics of the probe sheath was developed and the electron temperature and the plasma density which is found from the ion part of the probe characteristic (ion density) were measured in inductively coupled plasmas. The floating-type probe was compared with a single Langmuir probe and it turned out that the floating-type probe agrees closely with the single probe at various rf powers and pressures. The ion density and electron temperature by the floating-type probe were measured with a film on the probe tip coated in  $\text{CF}_4$  plasma. It is found that the ion density and electron temperature by the floating-type probe were almost the same regardless of the coating on the probe tip while a single Langmuir probe does not work. Because the floating-type probe is hardly affected by the deposition on the probe tip, it is expected to be applied to plasma diagnostics for plasma processing such as deposition or etching. © 2007 American Institute of Physics. [DOI: 10.1063/1.2204352]

## I. INTRODUCTION

Because Langmuir probes are relatively simple, they are used widely to measure plasma parameters such as the electron temperature ( $T_e$ ), the plasma density, the plasma potential, and other parameters in many plasma devices.<sup>1-5</sup> However, the Langmuir probe cannot be applied unless probe cleaning techniques are used to plasma diagnostics for etching and deposition plasmas because the metal tip of the probe can be coated or etched.

There have been some trials to overcome the weakness of Langmuir probes. Oliver and Clements had developed the radio frequency floating double probe.<sup>6</sup> They operated the double probe in the megahertz range and measured the sheath capacitance and the resistance of the cylindrical probe which give the electron density and the electron temperature. Because the operating frequency is high, if the contamination thickness is sufficiently smaller than the sheath thickness, this probe works well in spite of the contamination of the probe tip. To determine the exact electron density and the temperature with this probe, we should know exactly the density and temperature dependence of the sheath capacitance for a given probe geometry. There have been other trials such as a cut-off probe or a hairpin probe using microwaves.<sup>7-10</sup> The cut-off probe has some limitations in the size of the reactor, and the hairpin probe shows about 30% higher density in comparison with the Langmuir probe.<sup>10</sup> Moreover, these probes cannot measure the electron temperature.

Godyak *et al.* developed a rf floating-type probe using the nonlinear characteristics of the probe sheath in rf plasma.<sup>11</sup> If the frequency applied to the probe is sufficiently high, the current from the plasma can flow through a non-conducting film on the probe as a displacement current even

though the probe is contaminated. This indicates that this type of probe can be one of the methods to overcome the shortcoming of the Langmuir probe. The floating-type probe has been used to measure the electron temperature for a fast time resolution in the Tokamak plasma.<sup>12-14</sup> In the work of Boedo *et al.*,<sup>14</sup> they used a Pearson transformer to pick up the current which is not adequate at the processing plasma where the flowing current is much smaller than that of the Tokamak. Moreover the mutual inductance of the circuit and a Pearson transformer can induce a change in the sheath voltage drop, which results in the inaccurate measurement of plasma parameters.

In this work, a floating-type probe and its circuit applicable to the processing plasma are developed. A current sensing resistor and a differential amplifier (INA117) are used to measure the current, and the fast Fourier transform (FFT) is used to separate  $\omega$  and  $2\omega$  signals. A proper correction for the sheath voltage drop is also made for the exact measurement. With some modifications, we can get not only the electron temperature but also the plasma density. Because the plasma parameters with a floating-type probe have never been measured in the low temperature plasma, the measured results were compared with those of a single Langmuir probe (SLP) in order to check the reliability. For industrial applications, we also tested our floating-type probe by coating the probe tip in  $\text{CF}_4$  plasmas. In such a condition, the single Langmuir probe does not work. The floating-type probe with sufficiently high probe operating frequency is hardly affected by the contaminant deposition on the probe tip, and therefore, it has a potential to be applied to plasma diagnostics for processing plasmas such as deposition or etching plasmas.

## II. PRINCIPLES OF MEASUREMENT

When the electrons are in the Maxwellian distribution, the current flow through the probe tip, whose bias voltage is  $V_B$ , is given as in the following:<sup>15</sup>

<sup>a)</sup>Author to whom correspondence should be addressed; electronic mail: joykang@hanyang.ac.kr

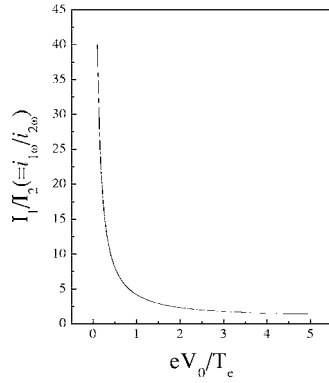


FIG. 1. Ratio of  $I_1/I_2$  as a function of  $eV_0/T_e$ . By measuring  $1\omega$  and  $2\omega$  currents, we can calculate the electron temperature.

$$i_{pr} = i^+ - i^- \exp[e(V_B - V_p)/T_e]. \quad (1)$$

Here,  $V_p$  is the plasma potential,  $T_e$  is the electron temperature, and  $i^+$  and  $i^-$  are the ion and the electron saturation currents. If the probe bias voltage is given as  $V_B = \bar{V} + V_0 \cos \omega t$ , then, from Eq. (1),  $i_{pr}$  can be written as

$$i_{pr} = i^+ - i^- \exp[e(\bar{V} - V_p)/T_e] \exp[eV_0 \cos \omega t/T_e]. \quad (2)$$

Van Nieuwehove *et al.* showed that  $i_{pr}$  can be expanded with modified Bessel functions  $I_k(z)$ ,<sup>13</sup> and is separated to dc and ac as shown in the following:

$$i_{pr} = i^+ - i^- \exp\left[\frac{e(\bar{V} - V_p)}{T_e}\right] I_0\left(\frac{eV_0}{T_e}\right) - 2i^- \exp\left[\frac{e(\bar{V} - V_p)}{T_e}\right] \sum_{k=1}^{\infty} I_k\left(\frac{eV_0}{T_e}\right) \cos(k\omega t). \quad (3)$$

In our experiments, we used the capacitor to block the dc, and therefore, the dc component of the  $i_{pr}$  should be zero,

$$i_{dc} = i^+ - i^- \exp[e(\bar{V} - V_p)/T_e] I_0(eV_0/T_e) = 0. \quad (4)$$

Therefore, the probe current becomes

$$i_{pr} = -2i^- \exp[e(\bar{V} - V_p)/T_e] [I_1 \cos(\omega t) + I_2 \cos(2\omega t) + \dots] = -2i^- \exp[e(\bar{V} - V_p)/T_e] (i_{1\omega} + i_{2\omega} + \dots). \quad (5)$$

Equation (5) shows that the currents of multiple harmonics are generated when the probe potential is oscillated with angular frequency  $\omega$ . Since the amplitudes of each harmonic current are functions of only  $T_e$  and  $V_0$ , the electron temperature can be obtained by comparing any two harmonic amplitudes.<sup>12,14</sup> The ratio of the amplitudes of the first and second harmonics becomes as in the following:

$$|i_{1\omega}|/|i_{2\omega}| = I_1(eV_0/T_e)/I_2(eV_0/T_e), \quad (6)$$

and we can determine the electron temperature by measuring  $1\omega$  and  $2\omega$  currents as shown in Fig. 1

The ion density can be calculated from Eqs. (4) and (5). From these two equations, the first harmonic of the probe current is given as

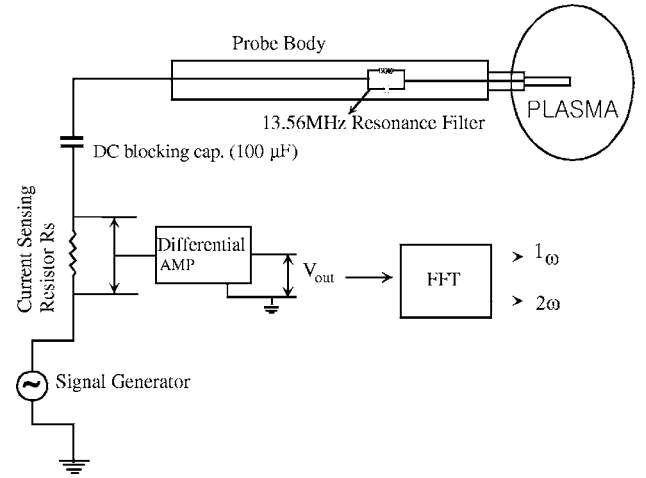


FIG. 2. A schematic diagram of the experimental setup.

$$i_{1\omega} = -2i^+ (I_1/I_0) \cos(\omega t) = -2(0.61en_i u_B A) (I_1/I_0) \cos(\omega t). \quad (7)$$

Here  $n_i$  is the ion density,  $u_B$  is the Bohm velocity, and  $A$  ( $\approx 4.7 \times 10^{-5} \text{ m}^2$ ) is the probe area. Therefore, by measuring the amplitude of the first harmonic current, the ion density can be calculated from Eq. (7) as in the following:

$$n_i = \frac{|i_{1\omega}|}{2(0.61eu_B A) I_1(eV_0/T_e)} I_0(eV_0/T_e). \quad (8)$$

In Eqs. (6) and (8), we assume that the voltage drop across the sheath is the same as the amplitude of the probe oscillating voltage  $V_0$ . However, as shown in Fig. 2, the presence of the current sensing resistor ( $R_s$ ), the dc blocking capacitor, and the 13.56 MHz resonance filter reduces the sheath voltage drop, and thus, a proper correction is needed to measure the temperature and the density exactly. To obtain the voltage drop across the sheath ( $V_{sh}$ ), we should know the impedance of the sheath. The sheath impedance can be given as an equivalent circuit of a resistor and a capacitor in parallel.

The sheath resistance ( $R_{sh}$ ) can be obtained by differentiating both sides of Eq. (1) which yields

$$di_{pr} = -\{i^-(e/T_e) \exp[e(V_B - V_p)/T_e]\} dV_B. \quad (9)$$

In our experiments, the small voltage oscillating around the floating potential is applied, and therefore, the probe current is very small and Eq. (1) can be rewritten as

$$i^+ \approx -i^- \exp[e(V_B - V_p)/T_e]. \quad (10)$$

From Eqs. (9) and (10), the sheath resistance around the floating potential is given as<sup>16</sup>

$$R_{sh}(V_f) = dV_B/di_{pr} \approx T_e J(ei^+) = T_e / (0.61e^2 n_i u_B A). \quad (11)$$

Figure 3 shows a calculated  $R_{sh}$  from Eq. (11) for various ion densities at 2 eV electron temperature.  $R_{sh}$  varies from 2 k $\Omega$  to 200  $\Omega$  as the ion density varies from  $10^{11}$  to  $10^{12} \text{ cm}^{-3}$ . Because we use a 100  $\Omega$  resistor for  $R_s$ , at high density region, we cannot neglect the effect of current sensing resistor. If we use a sufficiently low current sensing re-

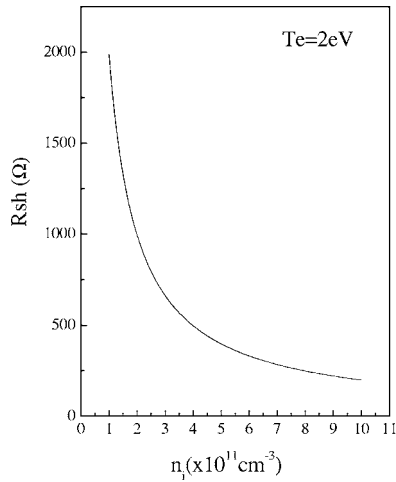


FIG. 3. Curve of calculated sheath resistance at various ion densities when  $T_e = 2$  eV.

sistor we can neglect the effect of the resistor; however, signal to noise ratio becomes worse.

The sheath capacitance of various probe geometries were studied by Crawford and Gard. When the time variation of the potential is too rapid for the ions to follow, and the sheath thickness is sufficiently small compared to the probe diameter, we can use a planar approximation, and by Child raw sheath, the sheath capacitance is given as follows:<sup>16</sup>

$$C_{\text{sh}}(V_f) = \left[ \exp\left(\frac{V_p - V_B}{T_e}\right) \right]^{1/2} \left[ \frac{m\pi T_e}{4M(V_p - V_B)} \right]^{1/4} \left( \frac{\epsilon_0 A}{\lambda_D} \right), \quad (12)$$

where  $m$  is an electron mass,  $M$  is an ion mass, and  $\lambda_D$  is a Debye length.

More general extension of the sheath capacitance to cylindrical geometry is given by Oliver and Clements. They applied the Langmuir-Blodgett formula for a cylindrical diode, and obtained the sheath capacitance of the cylindrical probe near the floating potential when the sheath length and the sheath area are  $s_0$  and  $A_{\text{sh}}$ , respectively,<sup>6</sup>

$$C_{\text{sh}}(V_f) = \left( \frac{s_0^2}{a^2 \Lambda} \right) \left[ \frac{m\pi T_e}{4Me(V_p - V_B)} \right]^{1/4} \times \left\{ \exp\left[ \frac{e(V_p - V_B)}{T_e} \right] \right\}^{1/2} \frac{A_{\text{sh}} \epsilon_0}{\lambda_D}. \quad (13)$$

Here,  $a$  is a probe radius,  $m$  is an electron mass,  $M$  is an ion mass, and  $\lambda_D$  is a Debye length.  $\Lambda$  in Eq. (13) is  $\partial\beta/\partial\gamma$ , where  $\gamma = \ln(a/s)$  and  $\beta = \gamma - 0.4\gamma^2 + 0.01917\gamma^3 - \dots$ .

Another model for the sheath capacitance in cylindrical geometry was predicted by Montgomery and Holmes.<sup>17</sup> If the potential of the probe is altered suddenly, the sheath surface charge density is also changed and about a time of  $1/f_i$ , where  $f_i$  is an ion plasma frequency, is required for the sheath to regain the steady state. If the potential oscillating frequency is higher than  $f_i$ , the distribution of ion density throughout the sheath is frozen, and only electrons move. In

such a case, the sheath in cylindrical geometry behaves like a coaxial cylindrical capacitor, and the capacitance is given as follows:

$$C_{\text{sh}}(V_f) = 2\pi\epsilon_0 l / \ln(s_0/a), \quad (14)$$

where  $l$  is the probe length.

The sheath capacitance near the floating potential calculated from Eq. (13) or Eq. (14) for our system is a few picofarad in our system, and therefore, the sheath reactance with several tens of kilohertz frequency is to the order of megaohm which is much larger than the sheath resistance. This indicates that the total impedance of the sheath is nearly the same as the sheath resistance. Because the dc blocking capacitance is very high, (100  $\mu\text{F}$ ), we can neglect the voltage drop across the capacitor. The impedance of the resonant filter is only a few ohms at 22.5 kHz frequency, and also can be negligible. Therefore, the voltage drop across the sheath becomes

$$V_{\text{sh}} \approx R_{\text{sh}}(V_f) V_0 / [R_s + R_{\text{sh}}(V_f)]. \quad (15)$$

The corrected equations for the electron temperature and the ion density are obtained by replacing  $V_0$  in Eqs. (6) and (8) with  $V_{\text{sh}}$ .

### III. EXPERIMENTAL SETUP

Figure 2 shows a schematic diagram of the experimental setup. Our system consists of a probe body, a signal generator, and a voltage difference amplifier. A tungsten probe tip, 15 mm in length and 1.0 mm in diameter, is connected in a series with a 13.56 MHz resonance filter that reduces 13.56 MHz noise. 4V<sub>p-p</sub> and 22.5 kHz sinusoidal wave is applied between the probe tip and the ground. The current flows from the signal generator, through the current sensing resistor and the probe tip, through the plasma, and back to the ground. The dc blocking capacitor is inserted in series to float the probe. The current is measured by measuring the voltage difference across the current sensing resistor. The amplitudes of  $\omega$  and  $2\omega$  currents can be found by fast Fourier transformation of the output voltage signal.

To compare our floating probe, a single Langmuir probe with a tungsten probe tip which is 0.1 mm in diameter and 10 mm in length is placed at the right side of the floating probe.<sup>18</sup> The SLP consists of a small measurement probe and floating loop reference probe with a 13.56 MHz resonance filter. The second derivative of the  $I$ - $V$  curve is obtained by numerical differentiation and numerical smoothing.<sup>19</sup> The measured second derivative  $I''_e$ , which is proportional to the electron energy probability function (EEPF)  $f(\epsilon)$ , is related to the electron energy distribution function (EEDF)  $g(\epsilon) = \epsilon^{1/2} f(\epsilon)$  as follows:<sup>15</sup>

$$g(\epsilon) = \frac{2m_e}{e^2 A} \left( \frac{2\epsilon}{m_e} \right)^{1/2} I''_e(\epsilon), \quad (16)$$

where  $\epsilon$  and  $A$  are the electron energy and probe area, respectively. The electron temperature can be calculated from the EEPF  $f(\epsilon)$ .<sup>15</sup> The ion density from the SLP was determined based on the Laframboise theory.<sup>20</sup>

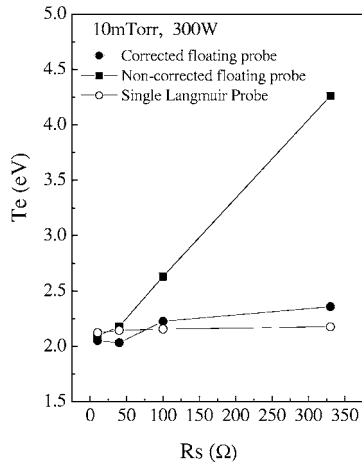


FIG. 4. The electron temperature against the current sensing resistance. The resistances are 10, 40, 100, and 330  $\Omega$ .

#### IV. EXPERIMENTAL RESULTS AND DISCUSSION

Figure 4 shows an electron temperature with (dark circle) and without (dark square) correction for the reduction of the sheath voltage drop due to the current sensing resistor at the 10 mTorr argon pressure and at rf power of 300 W. The open circles represent the SLP results. The sensing resistances were 10, 40, 100 and 330  $\Omega$ . When the sensing resistances are low (10 and 40  $\Omega$ ), with and without the sheath voltage correction results show nearly the same temperatures as the SLP. In this case, the sensing resistances are so much lower than the sheath resistance that almost all voltage is applied across the sheath, and therefore, the change in the sheath voltage drop is negligible. However, as the sensing resistance becomes higher, the change of the sheath voltage drop increases and the results without correction deviate from the SLP while corrected results agree closely with the SLP results. Therefore, noncorrection cases overestimate the electron temperature as shown in Fig. 4.

Figure 5 shows a comparison of electron temperatures and ion densities from the floating-type probe and the SLP at 50–600 W and at 20 mTorr argon pressure. The ion density increases almost linearly with rf power, as expected. Note

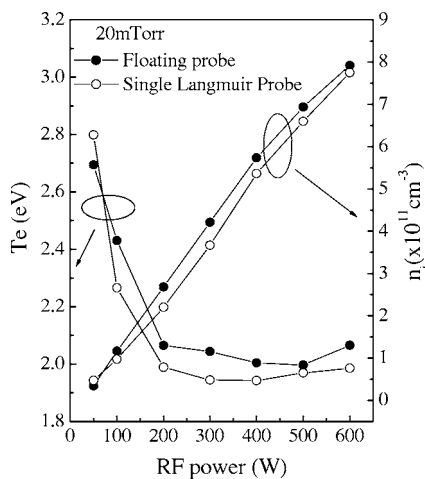


FIG. 5. The electron temperature and the ion density versus the rf power at 20 mTorr argon pressure.

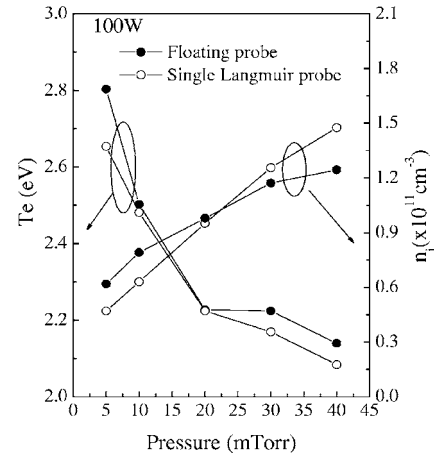


FIG. 6. The electron temperature and the ion density against the argon pressure at 100 W rf power.

that the electron temperature decreases with increasing input power.<sup>21,22</sup> This is caused by the multistep ionization effect.<sup>22,23</sup> Because the sheath resistance decreases with the increase in the ion density as expressed in Eq. (11), the correction for sheath voltage drop is essential to measure the accurate electron temperature and the ion density. In Fig. 5, the measured results from the floating probe show close agreements with those from the SLP within a few percent at various rf powers.

Figure 6 shows  $T_e$  and  $n_i$  from 5 to 40 mTorr argon pressure. From the particle balance between the total ionizations in volume and the total particle losses at the surface, increasing the pressure results in the decrease in the electron temperature. The electron temperatures from the two methods also show this well as shown in Fig. 6.

Because the floating-type probe operates near the floating potential, it measures only high energy electrons, i.e., the tail of the EEDF. At sufficiently low pressure, low and high energy electrons may have different temperatures, i.e., the electron energy distribution is in a bi-Maxwellian distribution. This is caused by the Ramsauer effect and the trapping of low energy electrons in ambipolar potential barrier.<sup>24</sup> In such case, the electron temperature from floating-type probe can be different from that of SLP. However, in our experiment, the bulk temperature is nearly the same as the temperature near the floating potential up to 5 mTorr, as shown in Fig. 7. At 5 mTorr, the plasma potential and floating potential are 16.28 and 7.07 eV, respectively. The low energy ( $\leq 5$  eV) electron temperature is 2.5 eV and the high energy ( $\sim 9$  eV) electron temperature is 2.6 eV. The electron temperature of high energy electrons is an important physical quantity because high energy electrons are mainly involved in the excitation or ionization processes.

The floating-type probe has a possibility that it can be applicable to real processing gas. Because the SLP measures the conducting current, the insulating film coated on the probe tip makes it difficult for the SLP to measure plasma parameters in real processing gas such as  $\text{CF}_4$ . To overcome this problem, continuous probe heating is needed. But continuous probe heating for cleaning causes an emission of thermal electrons, and as a result, can significantly perturb



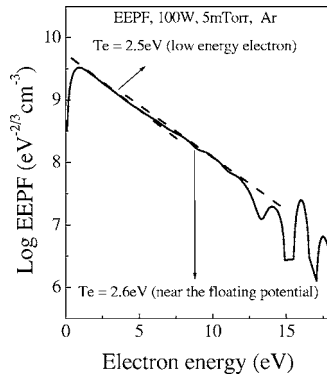


FIG. 7. The measured EEPF at 100 W and 5 mTorr argon pressure. The electron temperature of low energy electrons are nearly same as that of high energy electrons.

the discharge. However, if the operating frequency of the probe is sufficiently high, the current from the plasma can flow through a nonconducting film, and therefore, the floating-type probe works even though the probe tip is coated with an insulating film.

Figure 8 shows (a)  $I$ - $V$  curves and (b) EEPFs measured with SLP at 200 W rf power and 10 mTorr argon pressure. The solid lines are measured in the normal condition and dotted lines are measured with a film coated probe in  $\text{CF}_4$  plasma. We made a nonconducting film on the probe tip with a  $\text{CF}_4$  gas for 5 min, and then the measurements are done in pure argon gas. As expected, the coated SLP does not work. The electron current and the EEPF are significantly reduced

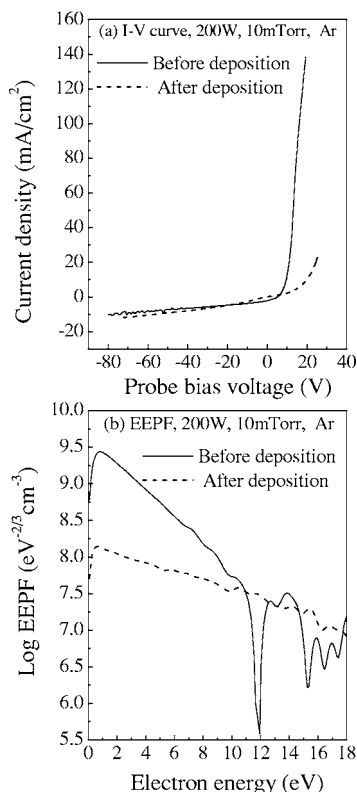


FIG. 8. The measured (a)  $I$ - $V$  curves and (b) EEPFs with SLP at 200 W rf power and 10 mTorr argon pressure. Solid lines are measured in the normal condition and dotted lines are measured with probe film coated in  $\text{CF}_4$  plasma.

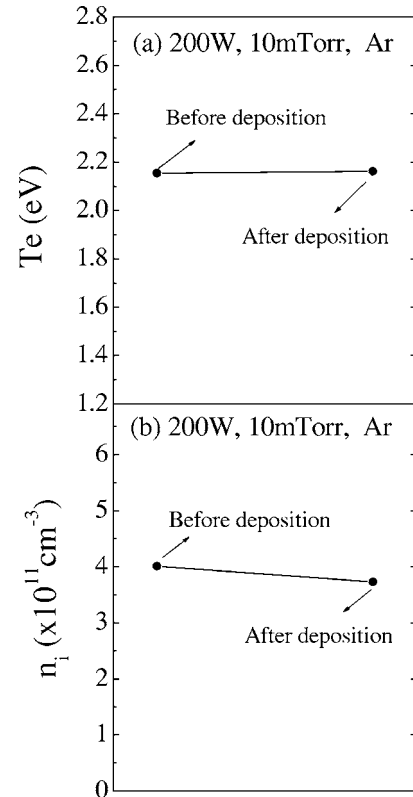


FIG. 9. The measured (a) electron temperatures and (b) ion densities with floating-type probe at 200 W rf power and 10 mTorr argon pressure before and after the film was coated on the probe tip.

compared with solid lines. This is because the film coated in  $\text{CF}_4$  plasma prevents the electron or the ion from being collected by the probe.

Figure 9 shows the (a) electron temperatures and (b) ion densities from the floating probe at 200 W rf power and 10 mTorr argon pressure. Points of “Before deposition” are measured in the normal condition and points of “After deposition” are obtained with the coated floating probe. The floating probe works well in spite of the deposition. However, if the coated film is very thick, the voltage drop across the sheath can be decreased a little, and this may result in the increase in the electron temperature and the decrease in the ion density. As shown in Fig. 9, the coated probe shows nearly the same temperature and density as with a noncoated one. This implies that the floating probe is not affected by the nonconducting film on the probe tip.

## V. CONCLUSION

We developed a floating-type probe and a circuit, and measured the electron temperature and the ion density using the nonlinearity characteristics of the sheath in the argon inductively coupled plasma (ICP). The main point of our probe is to measure the linear and nonlinear responses of current on applied ac voltage. With some corrections, the floating-type probe gives a close agreement in both the electron temperature and the ion density with the single Langmuir probe at various rf powers. When the rf power is increased from 50 to 600 W at 20 mTorr argon pressure, the measured electron temperatures show an accuracy of  $\approx 4\%$

with the single Langmuir probe, and the ion density is in the accuracy of  $\approx 10\%$ . Our probe also shows a good agreement at various pressures. When the pressure varied from 5 to 40 mTorr at 100 W input power, the measured electron temperatures and ion density show accuracies of  $\approx 3\%$  and  $\approx 16\%$ , respectively. This indicates that our probe works well in these power and pressure ranges. However, as can be seen in Eq. (11), the sheath resistance is inversely proportional to the ion density. If the plasma density becomes sufficiently high, the sheath resistance becomes small and the corrections for the 13.56 MHz resonance filter and dc blocking capacitor, which is not considered in our present model, are needed. Our probe gives the electron temperature and the ion density with high time resolution compared to the conventional Langmuir probe because of its high frequency operation.

We also confirm that the floating-type probe works well even in the situation where the probe tip is deposited in real processing plasma providing that the sheath resistance of the probe is sufficiently larger than the deposited insulating layer reactance. This can be satisfied if the applied voltage frequency is large enough. However, the frequency is limited by capacitive response of the probe, and therefore, the operating range of our probe is given as follows:

$$\frac{1}{\omega C_{\text{dep}}} \ll R_{\text{sh}} \ll \frac{1}{\omega C_{\text{sh}}}, \quad (17)$$

where,  $C_{\text{dep}}$  is a capacitance of the deposition layer and  $C_{\text{sh}}$  is a probe sheath capacitance. Since the floating-type probe is hardly affected by the deposition of the probe tip, it can be applied to processing plasma diagnostics such as deposition and etching.

There are some problems that should be overcome to apply the floating-type probe to the real processing plasma. One of them is an electronegative plasma problem. In the electronegative plasma, the negative ion density is usually larger than the electron density, especially at high pressure and low rf power. In such case, the probe current is composed of the positive ion current, the electron current, and the negative ion current instead of Eq. (1). Moreover, because the negative ions strongly reduce the velocity that is

required at the sheath edge, the Bohm velocity in Eq. (7) should be modified. Therefore, a further study for the electronegative plasma is required.

## ACKNOWLEDGMENTS

This work was supported by the Korea Research Institute of Standards and Science (KRISS). We appreciate the helpful advice of V. A. Godyak for this paper. This work was supported in part financially by MOCIE through the EIRC program (I-2004-0-074-0-00).

- <sup>1</sup>I. Langmuir and H. Mott-smith, *Gen. Electr. Rev.* **27**, 449 (1924).
- <sup>2</sup>F. F. Chen, in *Plasma Diagnostic Technique*, edited by R. H. Huddleston (Academic, New York, 1968).
- <sup>3</sup>N. Hershkowitz, in *Plasma Diagnostics*, edited by O. Auciello and D. L. Flamm (Academic, San Diego, 1989), Vol. 1.
- <sup>4</sup>J. A. Boedo, D. S. Gray, L. Chousal, R. Conn, B. Hiller, K. H. Finken, *Rev. Sci. Instrum.* **69**, 2663 (1998).
- <sup>5</sup>J. A. Boedo, D. S. Gray, L. Chousal, R. Conn, B. Hiller, and K. H. Finken, *Rev. Sci. Instrum.* **69**, 2663 (1998).
- <sup>6</sup>B. M. Oliver and R. M. Clements, *J. Appl. Phys.* **41**, 2117 (1970).
- <sup>7</sup>J. H. Kim, D. J. Seong, J. Y. Lim, and K. H. Chung, *Appl. Phys. Lett.* **83**, 4725 (2003).
- <sup>8</sup>R. L. Stenzel, *Rev. Sci. Instrum.* **47**, 603 (1976).
- <sup>9</sup>G. A. Hebner and I. C. Abraham, *J. Appl. Phys.* **90**, 10 (2001).
- <sup>10</sup>R. B. Piejak, V. A. Godyak, R. Gamer, B. M. Alexandrovich, and N. Sternberg, *J. Appl. Phys.* **95**, 3785 (2004).
- <sup>11</sup>V. A. Godyak, A. Kuzovnikov, and M. Khadir, *Radiotekhnika i Elektronika* **3**, 559 (1968).
- <sup>12</sup>D. L. Rudakov, J. A. Boedo, R. A. Moyer, R. D. Lehmer, and G. Gunner, *Rev. Sci. Instrum.* **72**, 453 (2001).
- <sup>13</sup>R. Van Nieuwehove and G. Van Oost, *Rev. Sci. Instrum.* **59**, 1053 (1988).
- <sup>14</sup>J. A. Boedo, D. Gray, R. W. Conn, P. Luong, M. Schaffer, R. S. Ivanov, A. V. Chernilevsky, and G. Van Oost, *Rev. Sci. Instrum.* **70**, 2997 (1999).
- <sup>15</sup>M. A. Liebermann and A. J. Lichtenberg, *Principles of Plasma Discharges and Material Processing* (Wiley, New York, 1994).
- <sup>16</sup>F. W. Crawford and R. Grard, *J. Appl. Phys.* **37**, 180 (1966).
- <sup>17</sup>R. M. Montgomery and R. A. Holmes, *Proceedings of the Fifth Biennial Symposium on Gas Dynamics*, edited by T. P. Anderson, R. W. Springer, and R. C. Warder, Jr. (Northwest University Press, Evanston, 1963).
- <sup>18</sup>V. A. Godyak, R. B. Piejak, and B. M. Alexandrovich, *Plasma Sources Sci. Technol.* **1**, 36 (1992).
- <sup>19</sup>J. I. Fernandez Palop, J. Ballesteros, V. Colomer, and M. A. Hernandez, *Rev. Sci. Instrum.* **66**, 4625 (1995).
- <sup>20</sup>J. G. Laframboise, Institute of Aerospace Studies, University of Toronto Report No. 100, 1966 (unpublished).
- <sup>21</sup>V. A. Godyak, R. B. Piejak, and B. M. Alexandrovich, *Plasma Sources Sci. Technol.* **11**, 525 (2002).
- <sup>22</sup>M. H. Lee and C. W. Chung, *Appl. Phys. Lett.* **87**, 131502 (2005).
- <sup>23</sup>M. H. Lee and C. W. Chung, *Phys. Plasmas* **12**, 073501 (2005).
- <sup>24</sup>V. A. Godyak and R. B. Piejak, *Phys. Rev. Lett.* **65**, 996 (1990).